

## Laser-interferometry study of oscillatory zoning in plagioclase: The record of magma mixing and phenocryst recycling in calc-alkaline magma chambers, Iztaccíhuatl volcano, Mexico

GRAHAM T. NIXON,\* T. H. PEARCE

Department of Geological Sciences, Queen's University, Kingston, Ontario, K7L 3N6, Canada

### ABSTRACT

Laser-interference microscopy has been used to study oscillatory zoning of plagioclase phenocrysts in calc-alkaline andesites and dacites of Iztaccíhuatl volcano, Mexico. Plagioclase crystals were analyzed in polished thin sections of hornblende dacites and andesitic "mixed" lavas characterized by disequilibrium phenocryst assemblages. Independent mineral and chemical data indicate that the latter rocks represent pre-eruptive mixtures of mantle-derived basaltic magmas and hornblende dacite magma residing in crustal reservoirs. Plagioclase zoning was investigated using "narrow-fringe" laser interferograms that give relative differences of An content ( $\Delta X_{An}$ ) across mineral grains with a routine detection limit of approximately 2.5 mol% and spatial resolution of about 2  $\mu\text{m}$ . Zoning profiles were digitized and calibrated by electron-microprobe analysis.

Plagioclase phenocrysts (0.2–7 mm) have euhedral to resorbed morphologies, well-developed oscillatory zoning ( $An_{66}$ – $An_{27}$ ), and andesine bulk compositions ( $An_{45}$ – $An_{35}$ ). The general style of zoning is oscillatory-even to weakly oscillatory-normal. Moderate-amplitude oscillations (10–3 mol% An) are superimposed on these first-order profiles. Major discontinuities in zoning ( $\Delta X_{An} = 10$ –33 mol%) coincide with resorption surfaces that are systematically overgrown by calcic plagioclase. Postresorption zoning is invariably normal and consistently steep in the most calcic zones; reverse zoning is comparatively rare. Textural features indicative of resorption include rounding of faceted growth forms, "angular unconformities," laterally discontinuous zones, and cusped to crenulate zone interfaces. Many peripheral sieve textures and internal zones of patchy extinction have developed by preferential dissolution within the (010) plane.

Resorbed phenocrysts in mixed lavas usually possess thin calcic rims ( $An_{66}$ – $An_{44}$ ) similar in composition to groundmass microlites ( $An_{62}$ – $An_{45}$ ) and Ca-rich zones overlying major internal discontinuities. Plagioclase populations in hornblende dacites differ primarily in their much reduced proportion of phenocrysts with calcic rims and resorbed outlines. Repeated exposure of phenocrysts to plagioclase-saturated and undersaturated melts has produced complex net-growth histories that can rarely be correlated among crystals.

The principal textural and compositional features of plagioclase may be explained by recycling of phenocrysts in open-system magma chambers. The dynamics of plagioclase evolution are consistent with mineral-melt equilibrium reactions in projected phase diagrams derived for low-pressure hydrous conditions. The most important recycling processes are believed to be liquid-state mixing, which promotes plagioclase dissolution, and *dynamic* fractional crystallization, which drives turbulently convecting hybrid liquids toward renewed precipitation of plagioclase.

### INTRODUCTION

Oscillatory zoning in igneous plagioclase has continued to merit detailed study as interest in the dynamics of magma chambers gains new impetus (e.g., Kuo and Kirkpatrick, 1982; Loomis and Welber, 1982; Anderson,

1984). Plagioclase is particularly well-suited for elucidating the magmatic evolution of orogenic rock suites because it typically constitutes the dominant phenocryst phase and is resistant to solid-state re-equilibration owing to the rather sluggish nature of CaAl-NaSi diffusive exchange at magmatic temperatures (Morse, 1984; Grove et al., 1984).

In the present study we have used laser-interference microscopy to document the internal features and compositional profiles of oscillatory-zoned plagioclase pheno-

\* Present address: Geological Survey Branch, Ministry of Mines, Energy, and Petroleum Resources, Parliament Buildings, Victoria, British Columbia V8V 1X4, Canada.

crystals in a suite of calc-alkaline andesites and dacites from Iztaccíhuatl volcano, Mexico. This technique offers a number of advantages over compositional profiles determined by the electron microprobe, for example, including better spatial resolution, which permits a clearer definition of zoning patterns and compositional discontinuities, and more rapid data collection. The micrometer-scale compositional stratigraphy of plagioclase phenocrysts in Iztaccíhuatl lavas provides an intricate history of magma chamber evolution. Recent mineral and chemical studies of Iztaccíhuatl (Nixon, 1987) have presented evidence for pre-eruptive mixing of dacitic magma residing in crustal reservoirs and primitive basaltic magma ascending from depth. We demonstrate below that many of the complex morphological features and systematics of plagioclase zoning in these rocks are consistent with open-system processes and reactions dictated by phase equilibria in the natural system.

### SAMPLE DESCRIPTION

Iztaccíhuatl (5286 m) is a major Quaternary volcano situated 60 km southeast of Mexico City (lat 19°10.7'N, long 98°38.5'W) in the central part of the Trans-Mexican volcanic belt. It forms part of the Sierra Nevada, a north-trending mountain range that defines the southeastern margin of the Valley of Mexico. Details of the geology and volcanic evolution of Iztaccíhuatl are provided by Nixon (1987) and Nixon et al. (1987).

Samples analyzed in this study were collected from two groups of flows within the Younger Andesites and Dacites of Iztaccíhuatl (<0.6 Ma) that were extruded from the southernmost summit vents of Rodillas and Pies. Two distinct rock types are represented: (1) hornblende dacites that contain phenocrysts of plagioclase (andesine-labradorite), hypersthene, edenitic to pargasitic hornblende, and minor ilmenite, titanomagnetite, biotite, and quartz enclosed in a hyalopilitic groundmass; and (2) andesitic "mixed" lavas characterized by unequilibrated phenocrysts of forsteritic olivine with inclusions of chrome spinel, bronzitic orthopyroxene, augite, edenitic-pargasitic hornblende, plagioclase (andesine-labradorite), biotite, quartz, ilmenite, and titanomagnetite set in an oxide-charged glassy groundmass. These disequilibrium phenocryst assemblages are interpreted to have formed by mixing of hornblende dacite and olivine-phyric basaltic magmas during magma-chamber recharge (Nixon, 1987).

Hornblende dacites, which represent the most evolved lavas of Iztaccíhuatl, mixed lavas, and primitive basaltic rocks erupted from vents on the flanks of Iztaccíhuatl and in the Valley of Mexico are plotted in MgO and Ni vs. SiO<sub>2</sub> diagrams (Fig. 1). The linear array of mixed lavas in the variation diagrams is consistent with an origin involving simple binary mixing of primitive basaltic and hornblende dacite magmas, as inferred from their mineral assemblages. The basaltic rocks plotted in Figure 1 are the closest natural analogues to calculated compositions of the basaltic component in mixed lavas (Nixon, 1987).

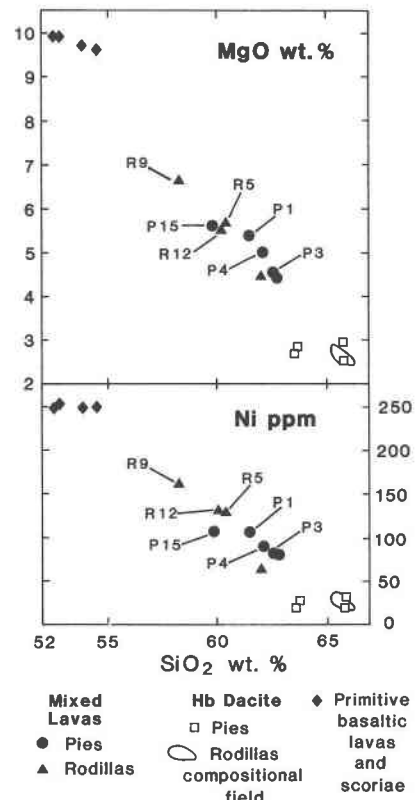


Fig. 1. Variation diagrams for MgO and Ni vs. SiO<sub>2</sub> for andesitic and dacitic lavas extruded from the Pies and Rodillas vents of Iztaccíhuatl and for primitive basalts erupted from vents on the flank of the volcano and in the Valley of Mexico. Mixed lavas analyzed in this study are labeled; sample notation corresponds to chemical analyses given in Nixon (1987).

### ANALYTICAL METHODS

#### Laser interference microscopy

The design of the laser-interference microscope and operating procedures have been described previously (Pearce, 1984a, 1984b). This investigation employed green light (514.5 nm) emitted by a Spectra-Physics 164 Ar-ion laser in the "narrow-fringe" mode of operation. Narrow-fringe laser-interference microscopy (NFLIM) provides an interferogram comprising a parallel set of light and dark fringes that run across a mineral specimen and contain quantitative information concerning the variation of refractive index, and hence composition, within the mineral. For a crystal of uniform thickness, relative differences in refractive index ( $\Delta n$ ) cause displacements of fringes or a "fringe shift" expressed by the equation  $n = S(\lambda/t)$  where  $S$  is the fringe shift ( $S = 1$  for a shift equal to the spacing between the dark reference fringes),  $\lambda$  is the wavelength of laser light used (514.5 nm), and  $t$  is specimen thickness (30  $\mu\text{m}$  for a normal thin section). Dispersion data relating the principal indices of refraction for plagioclase to composition in the An-Ab binary at the wavelength of the Ar-ion laser line are tabulated in Pearce (1984b). For a fringe shift of unity, the corresponding relative differences in An content ( $\Delta X_{\text{An}}$ ) are  $\alpha = 34.2$ ,  $\beta = 33.1$ , and  $\gamma = 32.0$  mol%. Thus, the fringe shift is only weakly dependent on optical orientation for a given plagioclase composition. The sensitivity of

the technique as applied to crystals examined in this study is estimated to be approximately 1/15 of a fringe shift or about 2.5 mol% An with an optimal spatial resolution of about 2  $\mu\text{m}$ .

Crystals selected for study were chosen from doubly polished thin sections, mounted on the laser-interference microscope, and photographed. In all, some 600 narrow-fringe photomicrographs of over 80 phenocrysts were examined. Representative fringe profiles were digitized in order to facilitate comparison between crystals. These digitized profiles are herein reproduced in graphical form.

#### Electron-microprobe analysis

The compositional profiles obtained by NFLIM were calibrated using an ARL-SEM-Q electron microprobe fitted with an energy-dispersive spectrometer and Tracor-Northern X-ray analysis system. Ten element analyses were performed simultaneously at selected points along each NFLIM profile using a 10- $\mu\text{m}$ -diameter electron beam, an accelerating potential of 15 kV, and a beam current of 0.08  $\mu\text{A}$ . A minimum of two analyses were averaged to obtain each calibration point, and the counting time for each analysis was 200 s. Materials used as standards were albite (Queen's University reference number S-122), labradorite (S-70), and a synthetic glass (S-204). X-ray intensities were corrected for matrix effects using the procedures of Bence and Albee (1968) and alpha correction factors of Albee and Ray (1970).

#### PLAGIOCLASE MORPHOLOGY AND COMPOSITION

Plagioclase is the principal phenocryst in Iztaccihuatl lavas. Phenocrysts range in size from 0.2 to 7 mm, though most average 2 to 4 mm and impart a distinctly hiatal texture to these lavas. External morphology varies from anhedral to euhedral and is typically diverse within a single thin section. Glomerocrystic intergrowths of two or three crystals are fairly common. All phenocrysts are oscillatory-zoned andesines with bulk compositions of approximately  $\text{An}_{35}$  to  $\text{An}_{45}$  (Nixon, 1987). Plagioclase phenocrysts form 6 to 34 vol% of the mode in hornblende dacites and 9 to 20 vol% of the mode in andesitic lavas.

#### LASER INTERFEROGRAMS: GENERAL FEATURES

When a mineral specimen is oriented appropriately in the laser-interference microscope, each dark interference fringe provides a graph of An content across the crystal, and collectively, the fringes form a two-dimensional image or interferogram of compositional variations in the plane of the polished section. Narrow-fringe interferograms of oscillatory-zoned andesine phenocrysts in Iztaccihuatl lavas are presented in Figure 2 together with drawings of selected fringe patterns. The zig-zag pattern of fringe displacement records oscillations superimposed on an overall even or normally zoned baseline. Fringe quality depends on specimen surface polish, crystal orientation, the presence and spacing of twin planes, fractures, and inclusions, and the geometry of zone interfaces. In some cases, it was necessary to construct profiles using more than one fringe trace in order to avoid defects (e.g., Figs. 2C, 2D). Discontinuities in the fringe trace mark a hiatus in composition, and these discontinuities are most sharply defined where the fringe trace is normal to a zone boundary and the inclination of the zone is perpendicular

to the plane of section. Fringe continuity was checked for the more significant displacements by measuring the inclination of zone boundaries, and the presence of a compositional hiatus was confirmed by a Becke line test. Ideally, fringes must intersect zone boundaries at right angles to avoid distortion.

The phenocryst shown in Figures 2A and 2B exhibits prominent discontinuities in the fringe trace that mark multiple resorption surfaces overgrown by more calcic plagioclase. Resorption in this particular phenocryst is identified by rounding of corners and gently curving surfaces that locally truncate inner oscillatory zones. These discontinuities correspond to fringe shifts of approximately 0.33–0.66S ( $\Delta X_{\text{An}} = 10\text{--}20$  mol%). Conspicuous calcic couplets mark maximum An contents with the exception of a thick (20  $\mu\text{m}$ ) normally zoned calcic rim ( $\text{An}_{58}\text{--}\text{An}_{47}$ ).

Figures 2C and 2D illustrate a phenocryst from a mixed lava with a profile that also contains distinctive pairings of peaks of maximum An content. Multiple resorption surfaces can also be recognized by rounding of corners, and many possess irregular embayments with inclusions of trapped glass. Calcic zones overlying resorption surfaces exhibit fringe displacements between 8 and 20 mol% An, and normal zoning is well-developed in the broad (35  $\mu\text{m}$ ) rim. Baseline curvature in this phenocryst is an artifact of thickness variation in the polished section. Using relations given above between section thickness and fringe displacement, the apparent fringe shift (0.5S) corresponds to a decrease in thickness from 30  $\mu\text{m}$  in the core to 20  $\mu\text{m}$  at the edge of this crystal.

#### INTERNAL FEATURES OF PHENOCRYSTS

Features observed within plagioclase phenocrysts are illustrated in Figures 3 to 5. Phenocrysts in mixed lavas and hornblende dacites exhibit many common characteristics. Oscillatory zoning is observed in all phenocrysts. Individual zones of uniform extinction range in width from  $\sim 1\text{--}80$   $\mu\text{m}$  on the same growth form, but the vast majority of zones have widths less than 30  $\mu\text{m}$ . Zone width may vary by a factor of 30 over a distance of some tens of micrometers on the same growth form and between (010) and other more rapidly growing interfaces. Some zones appear to be absent on (010). The broadest zones of uniform composition are invariably sodic, whereas the narrowest zones are either calcic or sodic.

#### Mixed lavas

Resorption surfaces punctuate the oscillatory zoning with no apparent systematic frequency. In most cases these hiatuses separate the corroded outer margin of Na-rich zones from more calcic plagioclase precipitated after the solution event. Resorption surfaces may be planar with slight rounding at the corners of crystals or curvilinear where corrosion is more advanced (Figs. 3A, 3C). These morphologies commonly alternate throughout the growth history and may pass laterally from one to the other. The

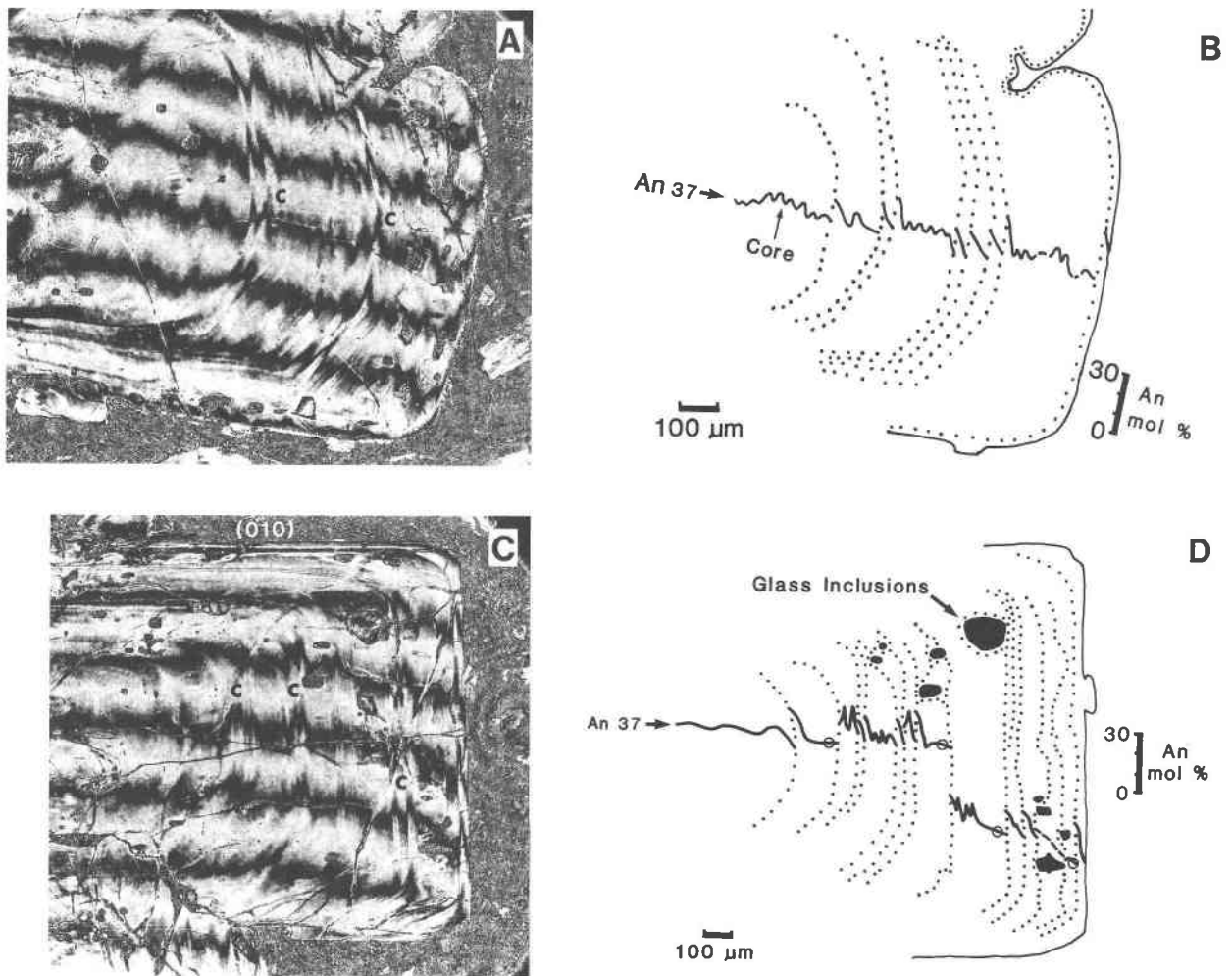


Fig. 2. (A, C) Narrow-fringe laser interferograms of plagioclase phenocrysts taken in Ar-ion light (514.5 nm) and (B, D) scale drawings of fringe profiles. Solid lines represent the fringe trace, and dotted lines are resorption surfaces. (A–B) Oscillatory-even zoning in phenocryst in hornblende dacite R3. Calcic couplets (c) mark peaks and maximum increases in An content ( $\Delta X_{An} = 15\text{--}20$  mol%) across discontinuities except for a single calcic peak at the normally zoned rim ( $An_{58}\text{--}An_{47}$ ). Section is cut  $\parallel$  (010) and passes through the approximate geometric center of the crystal. (C–D) Apparent normal zoning in phenocryst in mixed lava R5 caused by a gradual reduction in crystal thickness proximal to the edge of the thin section (beyond right margin of photo). Parts of two fringes are drawn for clarity (composite profile). Baseline curvature corresponds to an apparent 0.5 fringe shift or 17 mol% An. Probe analyses (open circles) are given for points of equal composition ( $An_{30}$ ). Peaks in An content occur as doublets ( $An_{47}$ ; cf. A–B) and the calcic rim ( $An_{50}\text{--}An_{30}$ ) has well-developed normal zoning with weak oscillations. Section cut  $\perp$  (010).

outer corroded margin of Na-rich zones may exhibit small-scale irregularities or localized cuspsate to U-shaped reentrants infilled by curving oscillatory zones or regions of patchy extinction (Figs. 3C and 2D). The latter comprise an irregular distribution of Ca-rich and Ca-poor plagioclase locally accompanied by inclusions of trapped glass. The most recent resorption surface commonly occurs within 10–30  $\mu\text{m}$  of the rim (Figs. 3B, 3D) and may be separated from a final overgrowth of calcic plagioclase by a region of dense inclusions or sieve-textured zone (Figs. 3E, 3F). The degree of rounding or roughness of the interface does not appear to have any influence on the composition of plagioclase crystallizing immediately after such corrosion events.

Other features diagnostic of resorption are shown in Figure 4. The width of sodic zones may pinch and swell laterally due to coalescence of solution surfaces, and calcic zones deposited on these surfaces may be locally discontinuous (Fig. 4A). Even the more planar resorption surfaces contain segments in which the width of the underlying sodic zone changes laterally, as can be readily seen by placing the eye parallel to the page and viewing Figure 4A along the strike of the two most prominent calcic zones near the rim of this phenocryst. Associated resorption features include tapering of sodic zones and “angular unconformities” (Fig. 4C). Oscillatory zoning may be interleaved with regions displaying textures that appear transitional toward patchy zoning and characterized by an

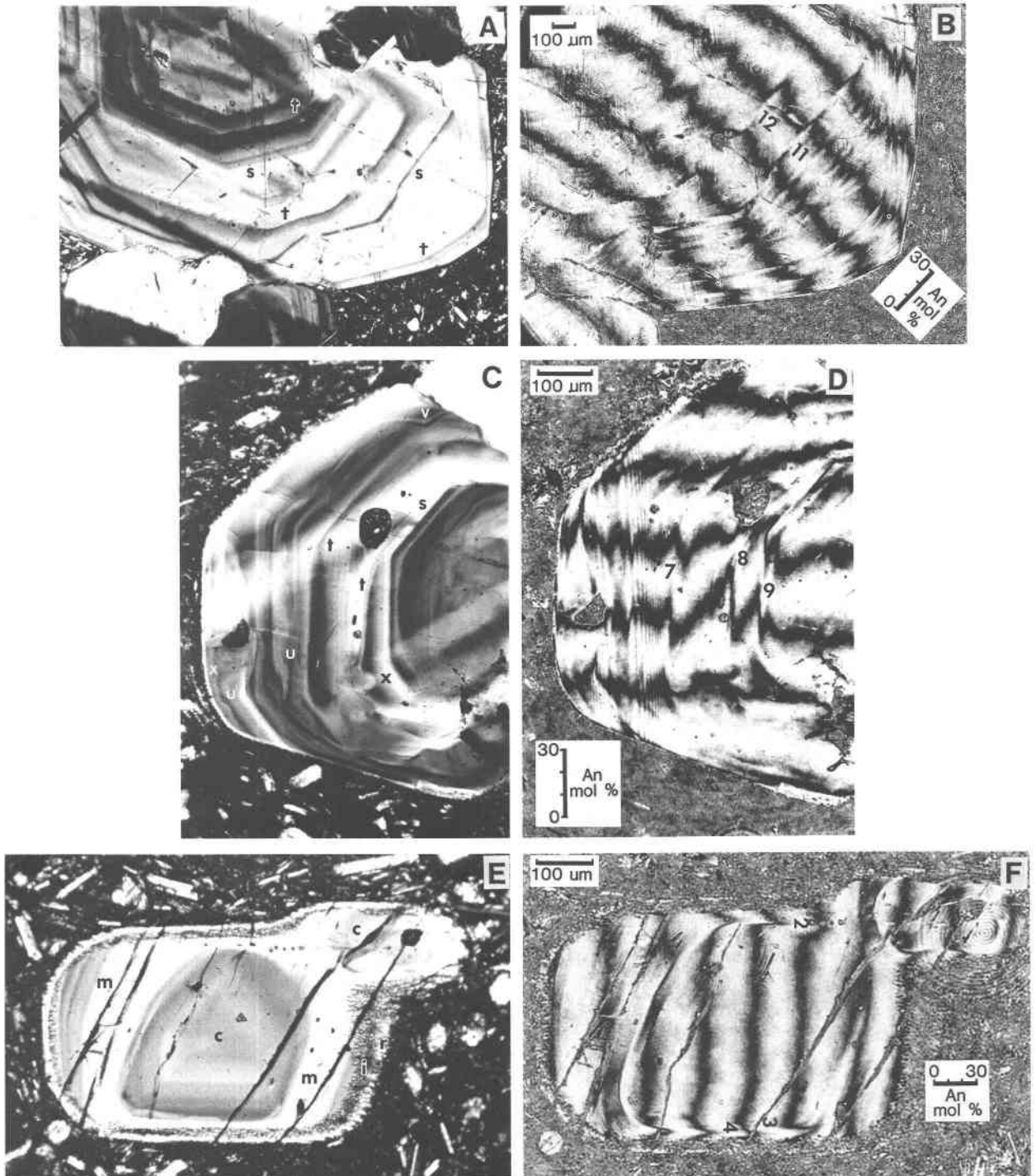


Fig. 3. (A, C, E) Internal features and compositional zoning in plagioclase phenocrysts observed under crossed polarizers and (B, D, F) matching narrow-fringe laser interferograms. (A–B) Calcic zones (at extinction in A) of variable width overlying solution surfaces with locally planar (s) or curvilinear (t) morphology. Discontinuities 11 and 12 are overlain by calcic zones of similar composition that exhibit a maximum displacement of 0.33 of a fringe shift ( $\Delta X_{An} \approx 11$  mol%). Note the fine-scale oscillatory zoning in the outer part of the crystal and the thin calcic rim. Section cut  $\parallel$  (010), mixed-lava profile P15-3, Fig. 9. (C–D) Calcic zones (white to pale gray) overlying resorption surfaces of variable morphology: planar (s), curvilinear (t), irregular (u), and cusped (v) locally exhibiting re-entrants (x). Discontinuities 7, 8, and 9 record fringe shifts of approximately 0.5, 1, and 0.66, corresponding to 16, 33, and 21 mol%  $\Delta X_{An}$  respectively. A thin, normally zoned calcic rim can just be discerned. Note the almost linear normal-zoning profiles in regions 7–8 and 8–9, and weak superimposed oscillatory zoning ( $\Delta X_{An} < 3$  mol%). Section cut  $\parallel$  (010), mixed-

inner smooth corrosion surface and irregular outer boundary.

A fairly common solution texture developed at the margins of phenocrysts is also portrayed in Figures 4A and 4B. Corrosion has fashioned a crenulated rim with etch pits excavated preferentially within the (010) plane that truncate inner oscillatory zones at variable depths. This fritted rim has subsequently been mantled by calcic plagioclase that has partially infilled preferentially oriented solution pits and trapped inclusions of glassy groundmass. An analogous texture shown in Figures 4C and 4D comprises rather coarse solution cusps with fritted inner margins—both structures preferentially etched  $\parallel$  (010)—that truncate relict oscillatory zones and resorption surfaces (see especially the central and lower part of the inclusion zone in Fig. 4C). Later crystallization produced a euhedral overgrowth of zoned (oscillatory-normal) calcic plagioclase exhibiting conspicuous edge thickening and a tendency toward skeletal growth. Trapped liquid eventually crystallized to a groundmass assemblage of plagioclase, pyroxene, and opaques.

#### Hornblende dacites

Variably spaced resorption surfaces in hornblende dacites also exhibit planar, curvilinear, cusped, or irregular morphologies; and tapering and coalescing zones and truncation of zones are also observed.

Textures at the rims of phenocrysts in hornblende dacites may be markedly diverse even within a single thin section. Figure 5A shows an intricately resorbed phenocryst affected by preferential dissolution  $\parallel$  (010) similar to features observed in mixed lavas (Fig. 4). A thin calcic rim exhibiting weakly developed dendritic outgrowths and re-entrant thinning overlies this resorption surface. The neighboring euhedral phenocryst likewise possesses a thin calcic overgrowth of comparable thickness and composition and has undoubtedly had a similar recent history, yet resorption is less severe. Coexisting phenocrysts may lack the outermost resorption surface and calcic rim. A euhedral phenocryst with an apparently homogeneous core and oscillatory-zoned mantle (Fig. 5B) exhibits near the margin of the crystal a sharp increase in An content that coincides with an inclusion-rich or sieve-textured zone with patchy extinction. The inner margin of this zone is preferentially corroded  $\parallel$  (010). The outer margin is normally zoned and separated from an oscillatory-zoned rim by a planar resorption surface. In this case, the rim composition is similar to that of the core ( $An_{38}$ ).

A euhedral phenocryst displaying oscillatory-even zon-

ing throughout is illustrated in Figure 5C. The margin of this crystal contains a sharply defined sodic trough ( $\Delta X_{An} \geq 10$  mol%) sandwiched between resorption surfaces that are flanked in turn by calcic zones. The style of zoning in these calcic zones varied conspicuously along strike. For example, the calcic zone bordering the inner margin of the trough in the central part of this phenocryst exhibits even or normal zoning, whereas in the lower part of the crystal, two distinct calcite peaks are evident, similar to the couplets observed in phenocrysts of mixed lavas (Figs. 2C, 2D) and other hornblende dacites (Figs. 2A, 2B). A related feature is shown in Figure 5D in which a narrow transition zone locally discernible along the inner margin of the trough marks a rapid continuous decrease in An content ( $\Delta X_{An} = 17$  mol%) after the resorption event.

In summary, internal features that appear to be diagnostic of resorption in these plagioclase phenocrysts include curvilinear zone boundaries and rounding of crystal corners, laterally coalescing zones, lateral truncation of zones ("angular unconformities"), cusped or irregularly crenulate zone margins, and sieve textures, especially those with inclusions preferentially oriented  $\parallel$  (010). Many such solution textures have been documented previously in natural feldspars (e.g., Bentor, 1951, Fig. 1; Vance, 1965; MacDonald and Katsura, 1965, Plate 1, Fig. 2; Rhodes et al., 1979, Fig. 2D; Kuo and Kirkpatrick, 1982, Figs. 1C, 2F) and synthesized in experimental runs (Lofgren and Norris, 1981; Tsuchiyama, 1985). The fine sieve textures in particular bear a striking resemblance to the "rough" interfaces illustrated by Tsuchiyama (1985, Fig. 3B) during dissolution of plagioclase in simple synthetic melts. However, preferential dissolution along crystallographic directions was not reported in his experimental products.

#### MICROLITE TEXTURES AND COMPOSITIONS

Plagioclase microlites (<0.2 mm) are the most abundant mineral constituent in the groundmass of Iztaccihuatl lavas. They occur as equant to lath-shaped crystals commonly exhibiting a hyalopilitic texture. The smallest laths typically display simple normal zoning, whereas the larger microlites and microphenocrysts (0.2–0.4 mm) usually possess more complex zoning patterns including at least one resorption surface.

Microlite morphology and zoning profiles are illustrated in Figure 6, which also shows their relationships to coexisting phenocrysts. A microlite lath with dendritic terminations and normal zoning with faint superimposed

←  
lava profile P3-3, Fig. 7. (E–F) Resorbed "double" core (c) succeeded outward by a normally zoned calcic mantle (m), an inclusion-rich rim (i), and an outer calcic overgrowth (r) largely free of inclusions. Note truncation of oscillatory zones in core and outer mantle. Discontinuity 2 records an outward increase in An content of almost a 0.5 fringe shift ( $\Delta X_{An} \approx 15$  mol%), whereas the cumulative displacement across discontinuities 3 and 4 on the opposite rim is only a 0.25 fringe shift and the composition of the mantle is barely more calcic than the core. Note the lateral variation in composition of the inner mantle. Section cut  $\parallel$  (010), mixed-lava profile P15-1, Fig. 9.

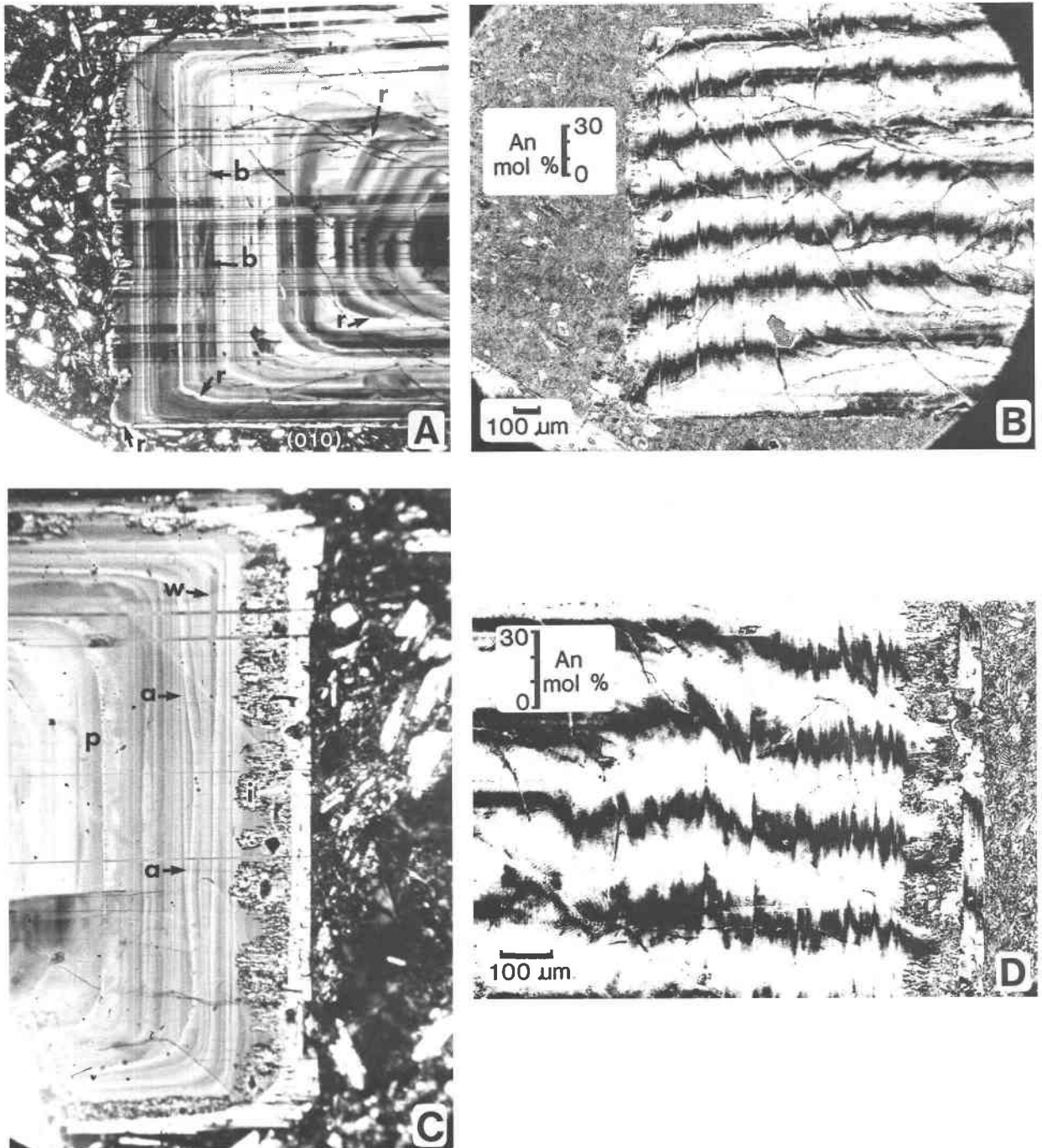


Fig. 4. (A, C) Internal features and zoning characteristics of plagioclase phenocrysts observed under crossed polarizers and (B, D) matching narrow-fringe laser interferograms. (A–B) Oscillatory-normal zoning in phenocryst in mixed lava P1. Calcic zones (white to pale gray) commonly overlie planar to curvilinear resorption surfaces. Note rounding of corners (*r*), laterally discontinuous bifurcating zones (*b*), and pronounced alignment of calcic plagioclase and trapped groundmass infilling dissolution pits in the rim that lie within the (010) plane. Maximum change in composition across a resorption surface is 20 mol%  $\Delta X_{An}$ , and baseline curvature is 15 mol%  $\Delta X_{An}$ . Section cut nearly  $\perp$  (010), profile P1, Fig. 9. (C–D) Oscillatory zoning in phenocryst of mixed lava P3. Sodic zones are near extinction in C. Core morphology includes angular unconformities (*a*), tapering of zones (*w*), and an area of patchy extinction (*p*) with localized concentrations of minute inclusions along its inner margin, and features present in A. A cusped inclusion-charged rim (*i*) is preferentially corroded  $\parallel$  (010) and truncates earlier oscillatory zoning and resorption surfaces. An outer calcic overgrowth ( $An_{60}$ ) exhibits oscillatory zoning and edge thickening suggestive of rapid growth. Section cut oblique to (010), profile P3-6, Fig. 7.

oscillations can be seen in Figure 6A (lowest microlite just beneath arrow). Since no internal resorption surface is present in this microlite, growth of this  $200\ \mu\text{m} \times 40\ \mu\text{m}$  lath must postdate the last resorption event to affect the neighboring phenocryst and thus be correlative with its thin ( $6\ \mu\text{m}$ ) calcic rim ( $\text{An}_{48}$ ). More complex relationships are evident in Figure 6B where a subequant microlite with a resorbed, normally zoned core has a calcic overgrowth ( $\Delta X_{\text{An}} = 20\ \text{mol}\%$ ) that exhibits steep normal zoning. This microlite has experienced at least one corrosion event that may be correlative with the final resorption surface at the rim of the nearby phenocryst.

Analyses of the cores of normally zoned microlites ( $15\text{--}40\ \mu\text{m}$  in width by  $100\text{--}300\ \mu\text{m}$  in length) in mixed lavas are as follows, in order of decreasing proportion of the basaltic end member in each mixed lava (approximated by the progression from mafic to salic compositions along the mixing trend in Fig. 1;  $n$  = number of microlites analyzed):

- R9:  $\text{An}_{60}\text{--}\text{An}_{47}$ ,  $n = 12$ ;
- P15:  $\text{An}_{62}\text{--}\text{An}_{56}$ ,  $n = 12$ ;
- R12:  $\text{An}_{56}\text{--}\text{An}_{48}$ ,  $n = 7$ ;
- R5:  $\text{An}_{56}\text{--}\text{An}_{45}$ ,  $n = 11$ ;
- P1:  $\text{An}_{57}\text{--}\text{An}_{50}$ ,  $n = 7$ ;
- P4:  $\text{An}_{61}\text{--}\text{An}_{52}$ ,  $n = 8$ ;
- P3:  $\text{An}_{56}\text{--}\text{An}_{48}$ ,  $n = 14$ .

Microlite compositions are systematically more calcic than the estimated bulk compositions of coexisting phenocrysts, but there appears to be no overall dependence between the composition of microlite cores and their position on the mixing trend in Figure 1. The most calcic microlite cores and most restricted range of zoning occur in P15, which has been rapidly quenched judging from the high proportion of glass in the groundmass. Some of the most sodic microlite cores are found in well-crystallized lavas with abundant plagioclase microlites (P1 and P3), but there are exceptions (P4). The significance of microlite compositions is examined further below.

### INCLUSIONS

Plagioclase phenocrysts contain inclusions of hypersthene, hornblende, opaque oxides, apatite, and residual liquid in various stages of crystallization. The latter phase forms inclusions of dark gray to colorless glass ( $2\text{--}200\ \mu\text{m}$  across)  $\pm$  vapor bubbles ( $<120\ \mu\text{m}$ ) to virtually holocrystalline groundmass (plagioclase + hypersthene + augite + Fe-Ti oxides + minor glass). These inclusions are commonly arranged in concentric zones comprising spherical to rectangular individual cells or irregular interconnected channelways (referred to as "coarse sieve texture," e.g., Figs. 2C, 2D), or they occur as fine elongate inclusions preferentially oriented  $\parallel$  (010) ("fine sieve texture," e.g., Figs. 4A, 4B) or as combinations of both (e.g., Figs. 4C, 4D). Sieve textures at phenocryst margins commonly truncate internal stratigraphy and in these cases are unequivocally related to dissolution (e.g., Figs. 3E and 4). Here, inclusions extend across the compositional hia-

tus and appear to have developed as re-entrants that became entombed by later growth. Glassy inclusions occurring well within phenocrysts are usually set in a base exhibiting patchy extinction due to subtle variations in plagioclase composition. Patchy zoning in some phenocrysts may develop during slower cooling within the magma chamber that thereby allows time for dissolution pits to become more completely infilled by subsequent plagioclase crystallization from the bulk melt or trapped liquid, or alternatively, from reactive interchange of plagioclase components at the walls of inclusions. In some cases, the origin of inclusion zones appears to be ambiguous and may be linked to either cellular growth during transient conditions of supersaturation (e.g., Anderson, 1984) or resorption (e.g., Vance, 1965; Tsuchiyama, 1985).

### PHENOCRYST ZONING PROFILES

Zoning profiles of plagioclase phenocrysts in Iztaccíhuatl lavas are presented in Figures 7 to 9 and summarized in detail in Appendix 1. Each profile represents a cross section through a different phenocryst, some of which have been illustrated in preceding photomicrographs (profiles referenced in captions to Figs. 3–6). Electron-microprobe analyses, represented as dots in Figures 7 to 9, provide absolute control on plagioclase compositions, and relative differences between control points are in good agreement with fringe patterns.

As noted previously, the overall style of zoning is oscillatory-normal or oscillatory-even, occurrences of reverse zoning over distances greater than a few tens of micrometers are extremely limited, and all major discontinuities correspond to resorption surfaces of variable morphology. The zoning profiles of phenocrysts in mixed lavas and hornblende dacites show no systematic differences, and their salient features will be described together.

### Phenocryst rims

Clear calcic rims ( $3\text{--}50\ \mu\text{m}$  thick) occur on practically all phenocrysts in mixed lavas but are much less common in hornblende dacites, generally forming  $<5\%$ , and in rare cases reaching  $50\text{--}60\%$  (e.g., R1), of the plagioclase population. Zoning at the rim is invariably normal or oscillatory-normal and commonly steep, and phenocrysts in mixed lavas may develop dendritic offshoots into the groundmass. The average width of normally-zoned calcic overgrowths tends to be greater in silicic mixed lavas than in mafic mixtures (e.g., profiles P1 and P4 vs. R9 and P15, Fig. 9). The broadest rims tend to have better developed oscillations ( $\Delta X_{\text{An}} = 7\ \text{mol}\%$ ), and no simple relationships are apparent between rim thickness or composition and the extent of zoning.

The composition of the inner rim at discontinuity 1 is highly variable ( $\text{An}_{66}\text{--}\text{An}_{30}$ ) and appears to be independent of the thickness or presence of an underlying inclusion-rich zone and the composition of the substrate on which it grew. The outer rims of phenocrysts vary in composition from  $\text{An}_{61}$  to  $\text{An}_{30}$ . The bulk compositions



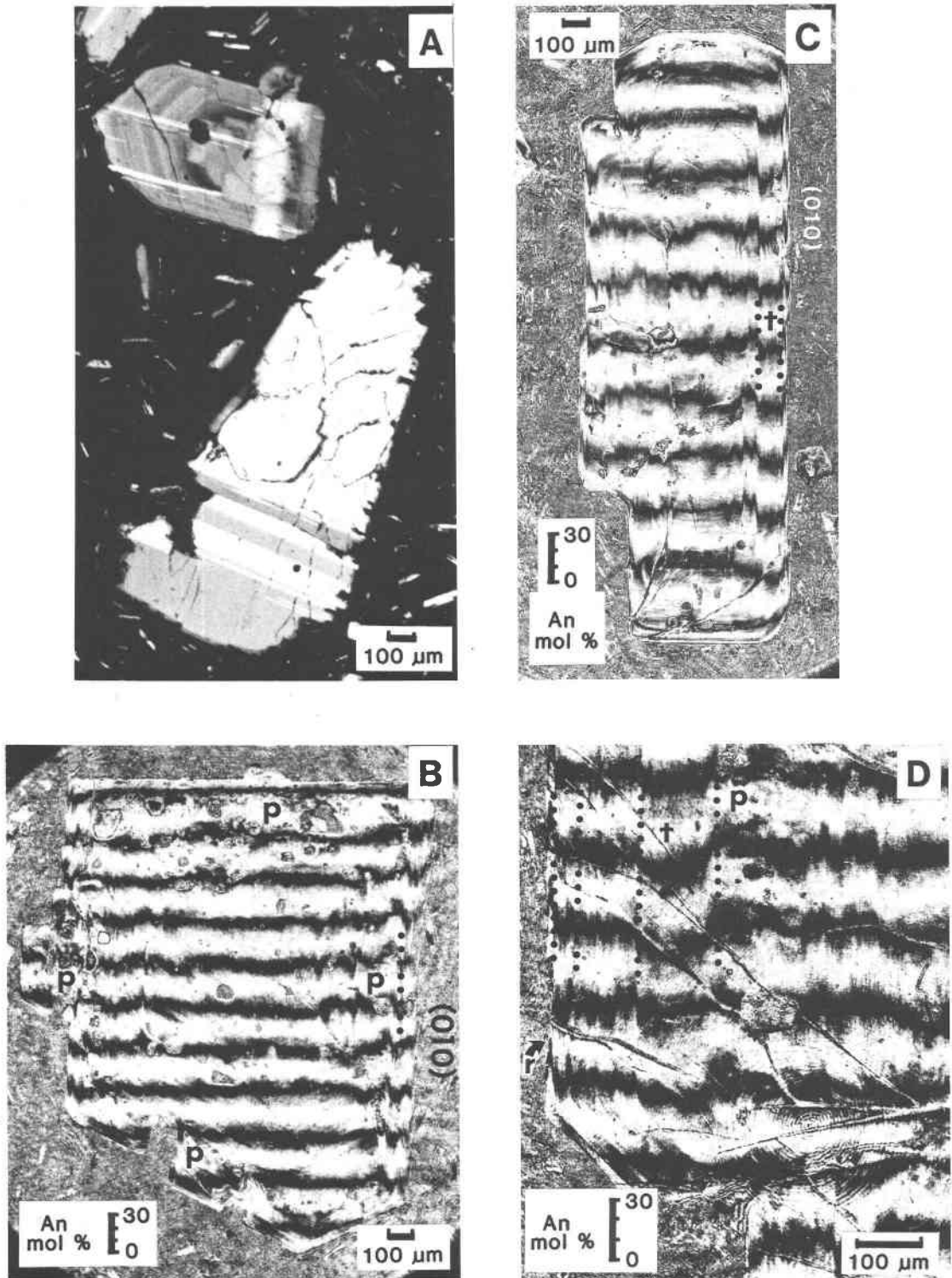


Fig. 5. Internal features and compositional zoning of plagioclase phenocrysts in hornblende dacites. (A) Juxtaposed euhedral and intricately resorbed andesine phenocrysts in R3 (crossed polarizers). Pronounced dissolution  $\parallel$  (010) occurs at the margin of the anhedral grain, and thin calcic rims are also present (only visible at lower edge of anhedral crystal as a dark gray ragged border). Narrow-fringe laser interferograms: (B) Euhedral phenocryst showing oscillatory-even zoning, an inner discontinuity (dotted) overlying an inclusion-rich region (p), and a rim similar in composition to the core. Section nearly  $\perp$  (010), profile R1-1, Fig. 8. (C) Phenocryst exhibiting an oscillatory-zoned sodic trough (t) flanked by resorption surfaces (dotted) and oscillatory-zoned calcic regions of like composition. Section cut  $\perp$  (010), profile R1-2, Fig. 8. (D) Margin of oscillatory-zoned phenocryst with a normally

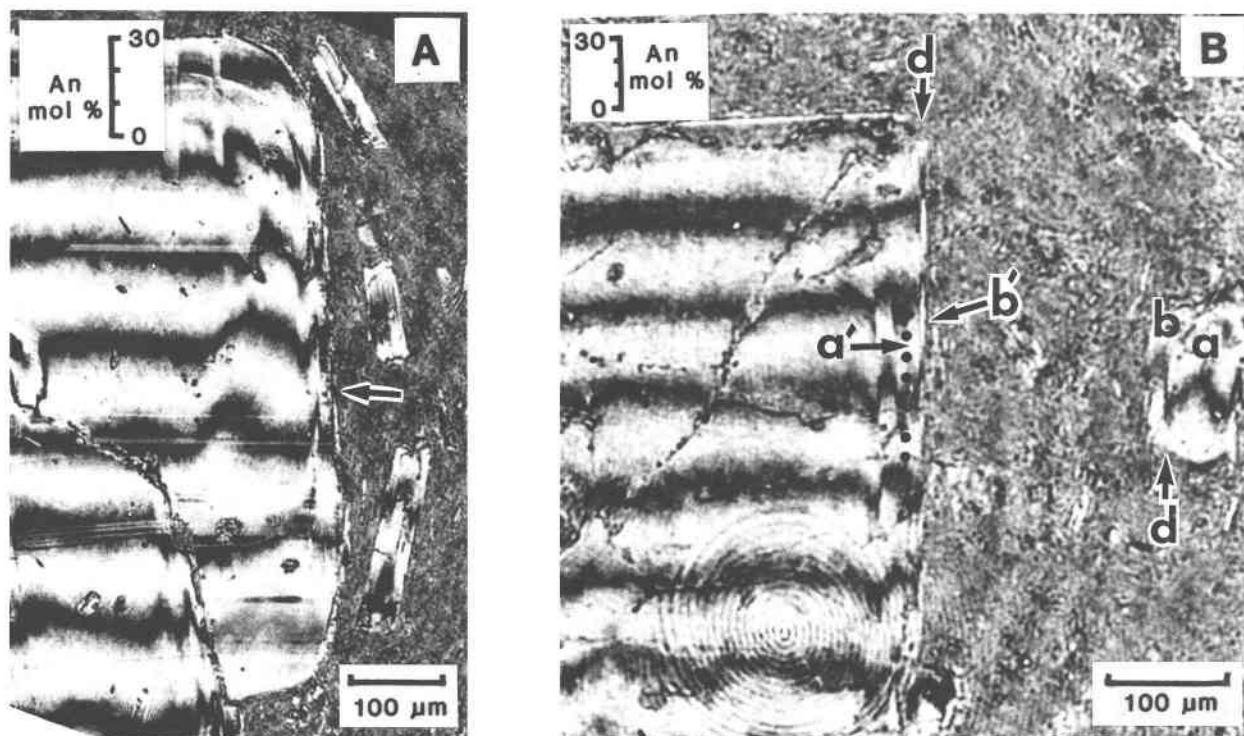


Fig. 6. Narrow-fringe laser interferograms showing phenocryst-microlite relationships. (A) Microlites exhibiting simple normal zoning with faint oscillations correlative with the thin outermost calcic rim of neighboring phenocryst. Arrow marks rim composition. Mixed lava P3; rim composition is equivalent to that of profile P3-4, Fig. 7. (B) Permissive correlation of normally zoned microlite core (a) and calcic rim (b) overlying a resorption surface (d) with zones (a', b') at the margin of a phenocryst in hornblende dacite R3.

of calcic overgrowths in mixed lavas are generally similar to groundmass microlite cores, but there are rare exceptions where anomalously sodic phenocryst rims persist metastably (e.g., P1 in Fig. 9; R5 in Figs. 2C, 2D). In hornblende dacites, overgrowths distinctly more calcic than bulk phenocryst compositions appear to be metastable owing to their typically low frequency of occurrence, the more silicic character of residual glasses, and general paucity of calcic microlites. In the latter lavas, there appears to be a continuum of phenocryst rim compositions extending from more than  $An_{60}$  to at least  $An_{30}$ .

#### Inclusion zones

Concentric zones (10–120 μm thick) of glassy inclusions ± vapor bubbles (sieve textures) are found near the margins and less commonly in the cores of phenocrysts. Sieve textures developed  $\parallel$  (010) commonly occur at the margins of phenocrysts in mixed lavas. Their inner border is a corrosion surface (discontinuity 1) and outer margin a constructional interface (normally zoned calcic rim).

Peripheral sieve textures occur in less than 5% of the phenocrysts in hornblende dacites and the majority of these crystals have well-rounded outlines, all support clear calcic overgrowths, and trapped glass is typically more mafic than the host groundmass glass.

#### Discontinuities

Discontinuities in phenocryst zoning profiles, identified as resorption surfaces, are almost invariably overgrown by plagioclase of more calcic composition with  $\Delta X_{An}$  ranging from as little as 3 mol% to as much as 33 mol%. Major discontinuities ( $\Delta X_{An} \geq 10$  mol%) are a characteristic feature of all zoning profiles and show no bias in distribution toward phenocryst cores or rims.

#### Postresorption zoning

Zoning immediately following resorption is generally normal or oscillatory-normal, and rarely even, reverse or oscillatory-reverse. Continuous normal zoning after resorption may be strikingly linear and practically as exten-

← zoned calcic rim (r), an inner region of patchy zoning with localized inclusions (p), and a sodic trough (t) bounded by resorption surfaces (dotted). Note the gradational inner margin of this trough compared to that in C. Section cut subparallel to (010), profile R3-2, Fig. 8.

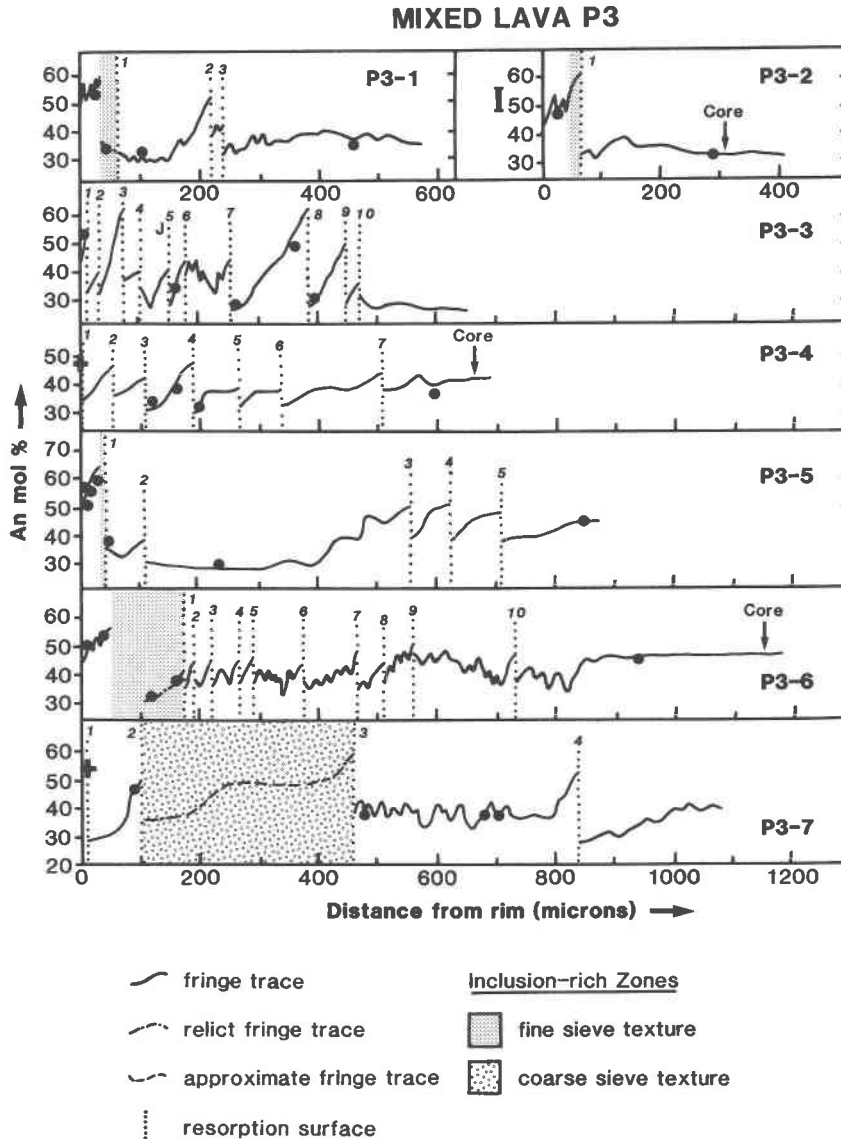


Fig. 7. Representative zoning profiles of plagioclase phenocrysts 1 to 7 in a single mixed lava (P3). Minor-amplitude ( $\Delta X_{An} < 3$  mol%), small-wavelength ( $< 5 \mu\text{m}$ ) oscillations locally visible in some of the interferograms may be superimposed on parts of these "smoothed" profiles. Discontinuities are numbered sequentially from the rim. Dots indicate the location of microprobe analyses (average of two determinations) used to calibrate the profiles. The bar symbol gives the range of core compositions for groundmass microlites in the rock, and a cross indicates the position of the fringe where its shape cannot be adequately resolved. J is the join in a composite profile constructed using more than one fringe trace.

sive as the entire range of plagioclase compositions (e.g., Figs. 3C, 3D). In general, steep normal zoning is a feature of the most calcic plagioclase compositions.

#### Correlation of profiles

The frequency of resorption surfaces in phenocryst interiors generally prevents firm correlations of zones between and even within crystals. For example, hornblende dacite profile R1-3 (Fig. 8) is symmetrical with respect to the number of discontinuities on either side of the core, but  $\Delta X_{An}$  is only 8 mol% at discontinuity 4 compared to

17 mol% at the plausibly correlative discontinuity 3 where postresorption zoning is steeper and starts at a more calcic plagioclase composition ( $An_{55}$  vs.  $An_{45}$ ). Profile R1-2 in the same thin section is more symmetrical in the style of zoning and initial postresorption compositions, but has an extra sodic shell not evident in R1-3. Asymmetric profiles exhibiting postresorption compositional differences and stratigraphic hiatuses are also evident in mixed lavas (e.g., P15-1, Figs. 9, 3E, 3F). These features are commonly caused by coalescence of resorption surfaces.

In attempting to correlate profiles, care was taken to

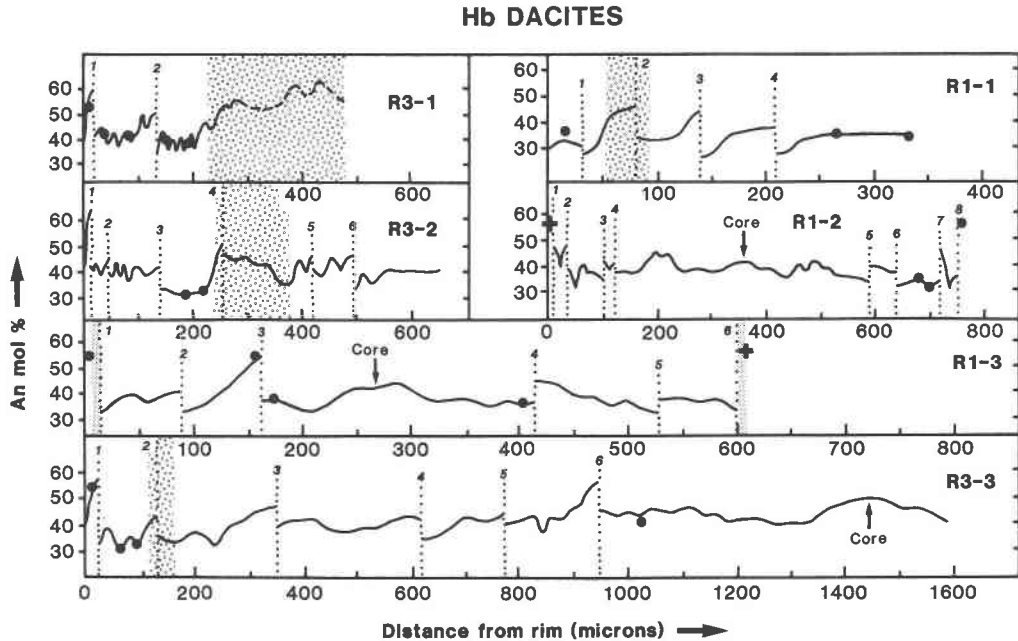


Fig. 8. Zoning profiles for plagioclase phenocrysts in hornblende dacites (R1 and R3). Symbols are the same as in Fig. 7. Discontinuities in profiles R1-2 and R1-3 are numbered sequentially from one rim to the other owing to uncertainties in across-grain correlation of zones. Profiles such as R1-1, which has a rim composition similar to the core, are underrepresented in this diagram.

allow for different profile orientations. Fringes running subparallel to (010) usually provide more complete zoning information than profiles oriented normal to (010). Even when this is done, the most reliable correlations among phenocryst zoning profiles in the same rock rarely extend beyond discontinuity 1.

#### Zoning systematics

The compositional profiles of plagioclase phenocrysts in Iztaccihuatl lavas are characterized by nonuniform oscillatory zoning punctuated by irregularly spaced major compositional discontinuities ( $\Delta X_{An} = 10\text{--}33\text{ mol}\%$ ). The discontinuous increase in An following each resorption event is a striking feature of phenocryst stratigraphy and one that is surely fundamental to magma-chamber processes. Similar discontinuous reverse zoning has been documented in numerous investigations of oscillatory-zoned plagioclase (see Smith, 1974) and in routine petrographic descriptions of orogenic volcanic rocks (e.g., Frey et al., 1984; Morrice and Gill, 1986), but we are unaware of any other study where major hiatuses following resorption form such an integral part of plagioclase crystallization history.

### INTERPRETATION OF RESULTS

#### Equilibrium vs. disequilibrium crystallization

Compositional zoning in magmatic plagioclase may be considered in terms of equilibrium or disequilibrium processes acting in systems of constant bulk composition.

Oscillatory zoning has been attributed to disequilibrium processes related to growth-induced compositional gradients in melt adjacent to a crystal interface, whereas major compositional hiatuses are often perceived to require sudden large changes in physical conditions (e.g., Loomis, 1982; Smith and Lofgren, 1983; and see Smith (1974) for reviews of earlier literature).

The small-amplitude oscillations ( $\Delta X_{An} < 3\text{ mol}\%$ ) near the limit of resolution in laser interferograms and coarser oscillations ( $\Delta X_{An} < 10\text{ mol}\%$ ) with wavelengths from several to a few tens of micrometers are compatible with the magnitude of variations commonly invoked for disequilibrium growth models (e.g., Sibley et al., 1976; Al-lègre et al., 1981; Loomis and Welber, 1982). In addition, minor corrosive discontinuities ( $\Delta X_{An} \approx 3\text{ mol}\%$ ) with similar relationships to the major resorption surfaces shown in the phenocryst zoning profiles (i.e., a calcic zone overlying resorbed Na-rich plagioclase) are evident in many crystals. For instance, the total number of solution surfaces that can be positively identified between point *b* and the rim of the phenocryst shown in Figure 4A is 16, corresponding to one corrosion event for every 22  $\mu\text{m}$  of net growth; and in Figure 4C between point *p* and the inclusion zone (*i*), there are 22 resorption surfaces or one solution event for every 14  $\mu\text{m}$  of net growth. Although this investigation is not specifically concerned with such small-scale features, we note that there are disequilibrium crystallization models that can potentially account for repeated growth-induced instability of plagioclase in hydrous melts (Loomis, 1982).

The irregularly spaced major compositional hiatuses

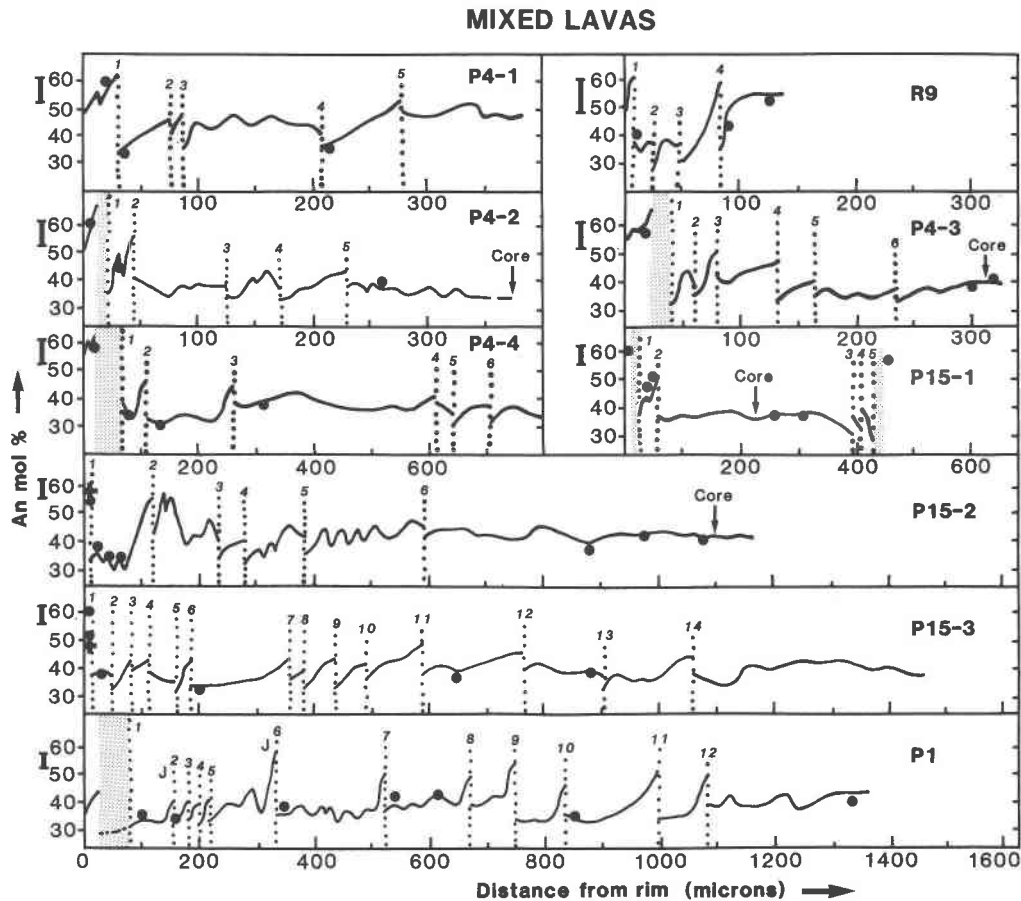


Fig. 9. Representative zoning profiles of plagioclase phenocrysts in mixed lavas (P1, P4, P15, and R9). Symbols are the same as in Fig. 7.

( $\Delta X_{\text{An}} = 10\text{--}33$  mol%) in phenocryst zoning profiles are almost as great as the width of the binary loop in the Ab-An system. Even if loop width were maintained in multicomponent systems, large variations in equilibrium plagioclase compositions require substantial changes in  $P$ ,  $T$ , and  $f_{\text{H}_2\text{O}}$ . For example, the isochemical pressure effect (anhydrous) on plagioclase composition calculated using the model of Ghiorso et al. (1983) is approximately 1.4 mol% An per kbar. Using equations given by C. H. Langmuir and G. N. Hansen (pers. comm., 1986) the pressure effect is slightly less (0.7 mol% An per kbar). Consequently, the amount of decompression needed to reproduce the major increases in An found in Iztaccíhuatl phenocrysts is unreasonably large because it requires magmas to begin their ascent at depths within the mantle that exceed the upper stability limit of plagioclase in natural melts. Similarly, the equilibrium isobaric temperature dependence of plagioclase compositions is estimated to be of the order of 1 mol% An per 10 °C and demands increases of up to several hundred degrees of account for observed increases of An in phenocryst zoning profiles. An equilibrium response of plagioclase compositions to temperature increases of comparable magnitude is an integral part of

magma mixing models discussed below. Numerical simulations of plagioclase crystallization presented by Loomis (1981, 1982) and experimental data evaluated by Anderson (1984, p. 671) yield comparable results and also suggests that isobaric fluctuations in  $\text{H}_2\text{O}$  content have no great influence on equilibrium compositions.

Disequilibrium growth processes triggered by undercooling or supersaturation generally result in a change in the partitioning of components between crystals and melt such that plagioclase compositions crystallizing from the melt become more albitic relative to compositions in equilibrium with the bulk melt (Lofgren, 1974; Loomis, 1982). Accordingly, nonequilibrium partitioning induced by supersaturation fails to account for the discontinuous increase in An observed in plagioclase phenocrysts. Loomis (1982) and Loomis and Welber (1982) considered that sharp increases in An content or resorption of plagioclase are most likely caused by increasing  $T$  or  $\text{H}_2\text{O}$  content of the melt in contact with crystals during disequilibrium growth. Although many equilibrium and disequilibrium crystallization processes and their probable interactions in isochemical systems remain to be tested quantitatively, many of the intrinsic features of plagioclase

class zoning profiles described in this study may be reconciled with equilibrium reactions predicted for open-system mixing and homogenization of basaltic and dacitic magmas as shown below.

### A magma-mixing model

Considering the geologic context of our samples, the textural and compositional attributes of plagioclase phenocrysts in Iztaccihuatl lavas can potentially place important constraints on the conditions and fractionation processes attending the hybridization of mafic and felsic magmas in crustal magma chambers. Accordingly, phenocrysts in mixed lavas are likely to yield information concerning the most recent pre-eruptive mixing event, whereas phenocrysts in hornblende dacites, which are intercalated with mixed lavas throughout the stratigraphy, may be expected to provide clues as to the nature of post-mixing differentiation.

The uniform bulk compositions of andesine phenocrysts in mixed lavas demonstrate that these crystals originated solely from the hornblende dacite end member. It is also clear from the rim textures of phenocrysts in mixed lavas that the last events to affect plagioclase were resorption and renewed crystallization of a more An-rich composition. From the remarkably systematic development of Ca-rich zones overlying resorption surfaces in the cores of these phenocrysts, it follows that these crystals have experienced multiple mixing events. Their characteristic oscillatory-even to weakly oscillatory-normal zoning profiles reflect the quasi-steady state dynamics of repeated cycles of resorption and crystallization at depth.

Phenocrysts in hornblende dacites have evidently had a similar net-growth history. Those with calcic rims were presumably involved in the most recent mixing event and have since been recycled back into the plagioclase-saturated environment of their hornblende dacite host.

### Phenocryst residence times

The morphology of andesine phenocrysts is primarily determined by the last dissolution event (i.e., discontinuity 1). Heterogeneous plagioclase morphologies within individual mixed lavas indicate that andesine phenocrysts have had variable residence times in plagioclase-undersaturated environments. Tsuchiyama (1985) has shown that euhedral crystals of sodic plagioclase immersed in plagioclase-undersaturated liquids in the system Ab-An-Di eventually become smaller and rounded as dissolution proceeds and simultaneously develop a fritted interface that may support sieve textures. Assuming that these results are valid for natural melts, andesine phenocrysts with smooth euhedral outlines record short residence times in undersaturated melts; rounded crystals have long residence times; and crystals with fritted margins or fine sieve textures have intermediate to long residence times depending on their gross external morphology.

Assuming that calcic microlites with simple normal zoning grew during eruption and that growth rates were

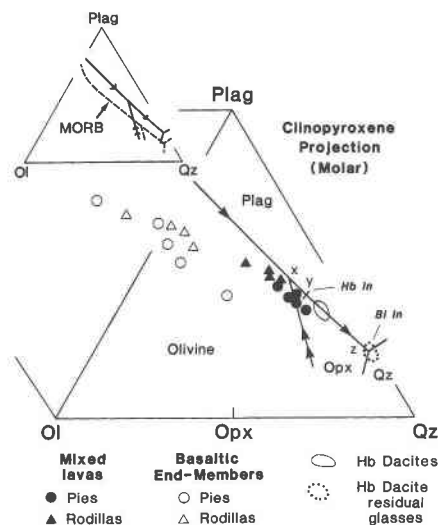


Fig. 10. Low-pressure liquidus phase relationships under hydrous conditions deduced for Iztaccihuatl magma chambers. Mixed lavas, hornblende dacites and their residual rhyolitic glasses, and basaltic end-member compositions (Nixon, 1987) are projected from clinopyroxene (Cpx) onto the plane olivine (Ol)-plagioclase (Plag)-silica (Qz) in the pseudoquaternary system Ol-Cpx-Plag-Qz. The projection scheme is from Grove et al. (1982). Opx = orthopyroxene; Hb = hornblende; Bi = biotite. The inset compares 1-atm liquidus phase relations for mid-ocean ridge basalts (MORB) from experiments of Walker et al. (1979) with those inferred for Iztaccihuatl. Points X, Y, and Z, and the construction of phase boundaries are explained in the text.

rather uniform, rim overgrowths of similar zoning style, width, and composition may be expected to occur on all phenocrysts. Rarely, phenocrysts in mixed lavas lack any optical indication of such overgrowths. A case in point is shown in Figures 2C and 2D. The rim of this phenocryst is 5–10 times broader than microlite half-widths and rims on neighboring phenocrysts and much more extensively zoned. This together with its faceted external morphology (prominent on the half of the crystal outside the field of view) implies that this crystal was incorporated in mixed magmas *after* microlite growth had begun and presumably concomitant with eruption. Extensive zoning at the rim of this crystal ( $An_{30}$ ) is interpreted to be a relict of its previous crystallization history in plagioclase-saturated hornblende dacite magmas. Were it not for quenching, this phenocryst would have developed a calcic couplet, similar to those observed within the core, recording its involvement in two closely spaced mixing events. Anomalous sodic rims on phenocrysts in other lavas (e.g., P1, Fig. 9) may likewise indicate extremely short residence times or disequilibrium growth in locally supersaturated liquids.

The variable residence times inferred for phenocrysts in plagioclase-undersaturated environments may be explained by andesine crystals being continuously added to hybrid magmas. The discontinuous reverse zoning yet continuous normal zoning of andesine phenocrysts is

compatible with progressive assimilation of hornblende dacite magma by evolving mafic melts, similar to some experimentally demonstrated interactions of basaltic and dacitic magmas (Kouchi and Sunagawa, 1985). We test the validity of these inferences in phase diagrams presented below and examine some further aspects of the magma-mixing model.

### Low-pressure phase relations

Liquidus phase relationships relevant to the origin of plagioclase textures and compositional variations are shown in Figure 10. The projection scheme employed is that of Grove et al. (1982), which reduces the number of components to six [olivine (Ol), clinopyroxene (Cpx), plagioclase (Plag), silica (Qz), orthoclase, and spinel] and is further simplified by projection into the quaternary system Ol-Cpx-Plag-Qz equivalent to the silica-rich part of the generalized basalt tetrahedron (Yoder and Tilley, 1962). The subprojection from Cpx is made onto the plane Ol-Plag-Qz and the join Ol-Plag represents the low-pressure thermal divide or critical plane. Plotted are mixed lavas, hornblende dacites, and their residual liquid (glass) compositions (obtained by microprobe analysis using a defocused beam), and the calculated compositions of basaltic end members (Nixon, 1987).

Depicted phase boundaries (Fig. 10) were deduced for the natural environment of crystallization and represent low-pressure hydrous conditions. The bulk compositions of hornblende dacites are assumed to represent liquids coexisting with plagioclase + orthopyroxene (Opx) + amphibole (Hb) + spinel (titanomagnetite) under the ambient conditions of Iztaccihuatl magma chambers. This assumption appears justified in view of the fact that modal proportions of phenocrysts in these lavas vary substantially, whereas bulk compositions remain uniform and show no effects that could be attributed to crystal accumulation. The quenched rhyolitic residual liquids of hornblende dacites are saturated with these solids plus biotite (Bi) and quartz (point Z in Fig. 10). The Hb-in-Cpx-out reaction point (Y) was inferred from the projected compositions of Cpx + Opx  $\pm$  Hb dacites from Iztaccihuatl not included in this study (Nixon, 1987). The olivine-melt reaction point (X) marks the projected composition of a Paricutin andesite (FP-16-52) that is multiply saturated in olivine + plagioclase + orthopyroxene + clinopyroxene at  $f_{\text{H}_2\text{O}} \approx 1$  kbar, equivalent to about 2–4 wt% H<sub>2</sub>O in the melt (Eggler, 1972; Grove et al., 1982). At these water contents, mineral-melt reaction curves occupy a narrow temperature interval, and their slopes ( $dP/dT$ ) are extremely steep (Eggler, 1972) such that multiple saturation of Iztaccihuatl magmas may well have occurred under conditions where  $P_{\text{total}} > f_{\text{H}_2\text{O}}$ . The Paricutin lava has compositional traits similar to the least siliceous Iztaccihuatl dacites and is essentially colinear with plagioclase-saturated phase boundaries for the more siliceous compositions. Note that these phase boundaries trend parallel to experimentally determined 1-atm cotectics for mid-ocean ridge basalts (Walker et al., 1979) but

are displaced toward higher plagioclase component. The shift in phase boundaries is related to the shrinkage of the plagioclase stability field at elevated  $f_{\text{H}_2\text{O}}$  combined with the higher alkalis of calc-alkaline magmas.

Grove et al. (1982, 1983) considered that phase boundaries and reaction points represented isobaric “pseudo-univariant” curves and “pseudo-invariant” points in the projected phase diagram. However, work in progress indicates that isobaric phase relationships in projection are sensitive to variations in bulk composition. For the compositions of interest here, the “cotectics” actually represent the mean trend of a narrow swath of subparallel curves, and “pseudo-invariant” points X, Y, and Z define an area in the projected phase diagram (see also Fujii and Scarfe, 1985). Nonetheless, the general topology of phase relationships appears valid and may be used to qualitatively convey the consequences of magma mixing and crystallization for plagioclase stability and composition.

The compositions of basaltic end members of mixed lavas (and their natural analogues erupted on the flank of Iztaccihuatl and in the Valley of Mexico) occupy the olivine primary phase volume and therefore project into the olivine stability field (Fig. 10). This is consistent with the mineral content of mixed lavas, which indicates that prior to mixing, basaltic magmas were near their liquidus (1250–1200 °C) and contained only phenocrysts of olivine and tiny euhedra of chrome spinel (Nixon, 1987). The residual liquids of hornblende dacites coexist with Plag + Opx + Hb + titanomagnetite + ilmenite  $\pm$  Bi  $\pm$  Qz and are therefore constrained to lie along the Plag + Opx (+ Hb) phase boundary between point Z and the field of bulk dacite compositions. Coexisting Fe-Ti oxide microphenocrysts and Ca-rich and Ca-poor pyroxenes resulting from the decomposition of amphibole indicate that equilibration temperatures in hornblende dacite magma chambers ranged from approximately 940 °C, below which augite reacts out and amphibole is stable (point Y in Fig. 10), to 880–820 °C where quartz and biotite appear (point Z; Nixon, 1987). The *bulk* compositions of mixed lavas occupy the olivine and orthopyroxene primary phase volumes and lie on mixing lines extending from the compositional field of hornblende dacites to their respective basaltic end members.

### Open-system processes and plagioclase evolution

From the topology of phase boundaries deduced above, it is clear that simple binary mixing of hornblende dacite and basaltic magmas produces hybrid *liquid* compositions that are out of equilibrium with plagioclase. Consequently, andesine phenocrysts originating in hornblende dacites that become entrained in mixed magmas will begin to dissolve, which explains the origin of resorbed plagioclase phenocrysts in mixed lavas.

Renewed precipitation of plagioclase requires fractionation of olivine and/or pyroxenes. Although direct evidence for fractional crystallization of mixed magmas is presented by skeletal terminations on olivine phenocrysts and normally zoned high-temperature ferromagnesian

silicates, gravitative settling of crystals during or after hybridization is not a viable mechanism for achieving plagioclase saturation in mixed magmas since their bulk compositions are controlled by mixing lines (Fig. 1). Nixon (1987) reconciled the petrographic and geochemical data by treating mixing and crystallization as concurrent differentiation processes operating during the progressive "assimilation" of hornblende dacite magma by hot basaltic magma ascending from depth. Three types of interaction were distinguished: (1) assimilation of low-temperature phenocrysts in the silicic end member; (2) blending of the rhyolitic residual liquids of hornblende dacite magma with rapidly evolving hybrid mafic melts; and (3) *dynamic* fractional crystallization in undercooled hybrid liquids. Hybridization of viscous dacitic and basaltic magmas was inferred to occur in a turbulently convecting interfacial region subject to thermal ( $\Delta T \approx 300$  °C) and compositional gradients (Kouchi and Sunagawa, 1985; Koyaguchi, 1985). Processes 2 and 3 above appear to be extremely efficient on the time scale over which magma-chamber recharge and eruption have taken place.

Elements of this concurrent mixing-fractional crystallization model that pertain to plagioclase evolution are shown in Figure 11. As basaltic magma becomes increasingly contaminated, bulk mixtures migrate along mixing lines toward the hornblende dacite end member as convective turbulence effectively maintains all solids in suspension. Evolving hybrid liquid paths are essentially governed by the relative rates of liquid blending and dynamic fractional crystallization. Continuous incorporation of low-temperature phenocrysts in plagioclase-undersaturated mafic liquids accounts for the different residence times inferred for variably resorbed andesine phenocrysts in mixed lavas.

The composition of plagioclase crystallizing from the melt cannot be inferred from these projections and has been estimated from the range of natural plagioclase solid solutions (Fig. 11). The fictive An content of the first plagioclase crystals to precipitate from evolving hybrid melts decreases with the degree of mixing and the amount of Ca-rich clinopyroxene fractionation prior to plagioclase appearance. In projections from olivine (not shown), primitive basaltic compositions lie close to the clinopyroxene + plagioclase (+ olivine) cotectic implying that Ca depletion by clinopyroxene, or the "augite effect" (Morse, 1979), has no significant influence on fictive plagioclase melt compositions—and hence initial plagioclase solid compositions—prior to cotectic crystallization, at least with respect to equilibrium phase relationships.

**Discontinuous Reverse Zoning.** Andesine phenocrysts in various stages of resorption acquire calcic overgrowths when fractionating hybrid liquids arrive at plagioclase-saturated cotectics (e.g., MFC evolutionary paths in Fig. 11), which explains the origin of major post-resorption increases in An content. The magnitude of the compositional hiatus depends on a number of factors: (1) hybrid liquids may have different evolutionary paths (e.g., variable extents of plagioclase + clinopyroxene fractiona-

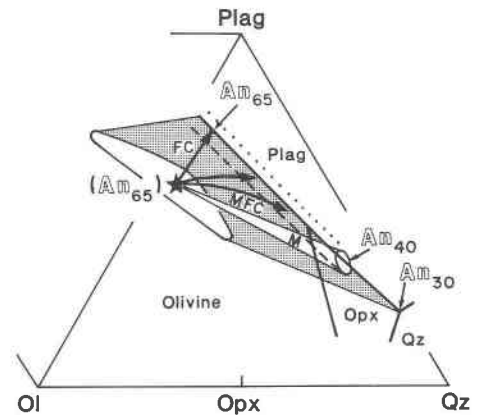


Fig. 11. Phase relations as in Fig. 10 showing the locus of simple binary mixtures (M) of hornblende dacite and a typical primitive basaltic composition, the fractional crystallization path for the mafic magma (FC), evolutionary paths for liquids continuously evolving by arbitrary combinations of mixing and fractional crystallization (MFC), and the total region accessible to MFC processes (shaded). Plagioclase compositions have been estimated for various melt compositions. The dashed line marks the approximate position of plagioclase-saturated phase boundaries at 1-atm (G. T. Nixon, unpub. data) and the dotted line represents a metastable cotectic appropriate for conditions of rapid cooling.

tion); (2) compositional gradients in hybrid melts; (3) incorporation of low-temperature phenocrysts at different stages of melt evolution; (4) basaltic end members with differing compositions (e.g., variable Ca/Na ratios or water contents); (5) suppression of plagioclase first appearance relative to clinopyroxene in rapidly cooled melts (e.g., Walker et al., 1976) as illustrated by a metastable shift in the plagioclase + clinopyroxene + olivine cotectic (Fig. 11); (6) disequilibrium partitioning of plagioclase components between crystal and melt associated with factor 5.

**Postresorption zoning.** Steep normal and often linear zoning profiles developed after resorption are invariably the case where plagioclase compositions exceed about An<sub>50</sub>. This style of zoning is consistent with crystallization of early-fractionating hybrid melts at high cooling rates (Lofgren, 1980). The occurrence of steep to shallow normal zoning, and rare reverse zoning, in more sodic postresorption plagioclase suggests that evolved hybrid liquids experienced more diverse thermal regimes and, on average, environments with slower rates of cooling were more accessible to randomly moving phenocrysts. The maximum extent of postresorption normal zoning is normally greater in phenocryst cores than in rim overgrowths that were quenched while magma mixing was in progress at depth.

**Oscillatory zoning.** In their apparently successful model for oscillatory zoning in plagioclase, Allègre et al. (1981) argued that low melt supersaturations are conducive to the development of oscillations. In this study, the persistence of oscillatory zoning in plagioclase phenocrysts at



depth, despite clear evidence in ferromagnesian silicates for strong undercooling and fractional crystallization of hybrid melts during magma mixing, is an apparent dichotomy that cannot be explained by reference to the pure An-Ab system. In the natural phase diagram (Fig. 11), primitive liquids evolving purely by fractional crystallization, for example, meet cotectics at a high angle of incidence and, at high cooling rates, are more likely to oversaturate equilibrium cotectics and become strongly supersaturated in plagioclase. Efficient liquid blending in early hybrids serves to constrain evolving melts to move more extensively through ferromagnesian-phase volumes and encounter plagioclase cotectics more obliquely, thereby promoting low melt supersaturations in plagioclase. Thus, open-system mixing is a mechanism that may be conducive to faceted growth and oscillatory zoning of plagioclase under conditions of strong undercooling.

**Phenocryst rims and microlite growth.** The complexities (1 to 6 above) governing discontinuous reverse zoning also account for the lack of correlation between microlite core compositions and the proportion of dacitic end member in the bulk compositions of mixed lavas. The slightly higher An contents of some inner rims relative to microlite cores may be related to early heterogeneous nucleation on pre-existing crystals versus delayed homogeneous nucleation in the melt under conditions of rapid cooling. The thicker phenocryst rims with locally well-developed oscillatory zoning presumably began their growth at depth. Normally zoned microlites nucleated during eruption because of an expansion of the plagioclase stability volume on decompression (Fig. 11). Supersaturation of hybrid liquids in plagioclase at this time explains the suppression of oscillatory zoning in microlites and in the thinner phenocryst rims and their locally dendritic offshoots.

**Phenocryst recycling.** Since hornblende dacites of rather uniform composition are intercalated with mixed lavas throughout the eruptive sequence, the volume of dacitic end member stored in crustal reservoirs appears to have greatly exceeded the volume of basaltic magma influx (Nixon, 1987). Thus, hybrid magmas evolve to the hornblende dacite bulk composition, unless quenched as mixed lavas, and residual liquids migrate down cotectics toward equilibrium with quartz, biotite, and sodic plagioclase (An<sub>30</sub>). As thermal and compositional gradients in magma chambers subside, gravitative settling of crystals may become important, but this does not affect late-stage liquid evolution paths that in either case are strongly controlled by low-pressure cotectics. Plagioclase phenocrysts involved in mixing and retained at depth ultimately re-equilibrate with rhyolitic residual liquids crystallizing sodic andesine. Therefore, phenocrysts in hornblende dacites that experienced a recent mixing event display variably resorbed morphologies and calcic rim compositions. Recycled phenocrysts exhibit the multiple internal calcic discontinuities followed by normal zoning to a quasi-steady-state "baseline" composition (An<sub>40</sub>-An<sub>30</sub>). Phenocrysts with calcic rims are eventually diluted by the

large population of euhedral andesine crystals that did not participate in recent mixing events. The preservation of some very thin calcic rims that are apparently out of equilibrium with rhyolitic residual liquids may be explained by relative rapid recycling of phenocrysts into a low-growth-rate environment coupled with the slow solid-state diffusive control of the exchange of plagioclase components between crystals and melt (Grove et al., 1984; Tsuchiyama, 1985). The low intercrystal correlation of phenocryst zoning profiles is a consequence of phenocryst-specific mixing and recycling mechanisms such as convective turbulence.

## CONCLUSIONS

Oscillatory zoning in andesine phenocrysts in the Younger Andesites and Dacites of Iztaccihuatl volcano, Mexico, is characterized by multiple major compositional discontinuities ( $\Delta X_{An} = 10\text{--}33$  mol%), marked by resorption surfaces of diverse morphology, succeeded by overgrowths of calcic plagioclase. We have interpreted plagioclase crystallization history as a quasi-steady-state response of recycled phenocrysts to repeated batch influx of primitive basaltic magma followed by mixing and crystallization in shallow-level dacitic magma chambers. The timing and severity of recorded events may change from phenocryst to phenocryst, but not the fundamental nature of the recycling processes. The most important open-system processes are believed to involve blending of residual liquids of contrasting composition accompanied by concurrent dynamic fractional crystallization of turbulently convecting hybrid magmas. The dynamics of plagioclase evolution are shown to be consistent with crystal-melt equilibria in projected phase diagrams derived for the low-pressure hydrous conditions of crystallization pertaining to Iztaccihuatl magma chambers.

Many of the textural and compositional features documented above for plagioclase phenocrysts in Iztaccihuatl lavas appear widespread in calc-alkaline rocks although the systematics of plagioclase stratigraphy have yet to be more thoroughly examined. In their study of mixed magmas at Lassen Peak in the Californian High Cascades, MacDonald and Katsura (1965) noted the occurrence of disequilibrium phenocryst assemblages, especially resorbed andesine phenocrysts with peripheral "clouded" zones and labradorite overgrowths similar in composition to groundmass microlites. However, they rejected a magma-mixing origin because these textures are so common in lavas with homogeneous matrices erupted throughout the Lassen region. At one point they inquired (MacDonald and Katsura, 1965, p. 480), "Are mixed magmas in which the mixing has progressed to the point that nearly all the evidence for mixing has been obliterated far more common than is realized?" In the light of our present study, we would be tempted to answer yes. In the hope of encouraging further work, we reiterate one of their statements: "These 'unhappy' feldspars . . . may be related to some of geology's most fundamental problems!"

## ACKNOWLEDGMENTS

This study was supported by Natural Sciences and Engineering Research Council of Canada Operating Grant A8709 and Infrastructure Grant A0656. It forms part of a continuing study of zoned crystals using a laser interference microscope (Canadian Patent No. 1,163,797; U.S. Patent Application No. 558,590, Laser Interferometer). The Laser Laboratory at Queen's University was funded by an NSERC New Research Idea Grant A5226, and NSERC Equipment Grants E6622, E1449, E5784, and E0296. Part of the initial research in this study was supported by grants from the Graduate School and the Advisory Research Committee, Queen's University. We thank P. L. Roeder for providing ready access to the electron-microprobe laboratory and Dave Kempson for analytical advice. Carol Luce did the drafting and keypunching of digitized data. Critical reviews of the manuscript by G. E. Lofgren, P. L. Roeder, and an anonymous reviewer are greatly appreciated. G.T.N. wishes to thank J. M. Dixon, H. Helmstead, and P. L. Roeder for securing funds for the completion of this manuscript.

## REFERENCES CITED

- Albee, A.L., and Ray, L. (1970) Correction factors for electron microanalysis of silicates, oxides, carbonates, phosphates and sulphates. *Analytical Chemistry*, 42, 1408-1414.
- Allègre, C.J., Provost, A., and Jaupart, C. (1981) Oscillatory zoning: a pathological case of crystal growth. *Nature*, 294, 223-228.
- Anderson, A.T., Jr. (1984) Probable relations between plagioclase zoning and magma dynamics, Fuego volcano, Guatemala. *American Mineralogist*, 69, 660-676.
- Bence, A.E., and Albee, A.L. (1968) Empirical correction factors for the electron microanalysis of silicates and oxides. *Journal of Geology*, 76, 382-386.
- Bentor, Y.K. (1951) On the formation of cloudy zones in plagioclases. *Schweizerische Mineralogische und Petrographische Mitteilungen*, 31, 535-552.
- Eggler, D.H. (1972) Water-saturated and undersaturated melting relations in a Parícutín andesite and an estimate of water content in the natural magma. *Contributions to Mineralogy and Petrology*, 34, 261-271.
- Frey, F.A., Gerlach, D.C., Hickey, R.L., Lopez-Escobar, L., and Muni-zaga-Vallavicencio, F. (1984) Petrogenesis of the Laguna del Maule volcanic complex, Chile (36°S). *Contributions to Mineralogy and Petrology*, 88, 133-149.
- Fujii, T., and Scarfe, C.M. (1985) Composition of liquids coexisting with spinel lherzolite at 10 kbar and the genesis of MORBs. *Contributions to Mineralogy and Petrology*, 90, 18-28.
- Ghiorso, M.S., Carmichael, I.S.E., Rivers, M.L., and Sack, R.O. (1983) The Gibbs free energy of mixing of natural silicate liquids: An expanded regular solution approximation for the calculation of magmatic intensive variables. *Contributions to Mineralogy and Petrology*, 84, 107-145.
- Grove, T.L., Gerlach, D.C., and Sando, T.W. (1982) Origin of calc-alkaline series lavas at Medicine Lake volcano by fractionation, assimilation, and mixing. *Contributions to Mineralogy and Petrology*, 80, 160-182.
- Grove, T.L., Gerlach, D.C., Sando, T.W., and Baker, M.B. (1983) Origin of calc-alkaline series lavas at Medicine Lake volcano by fractionation, assimilation, and mixing: Corrections and clarifications. *Contributions to Mineralogy and Petrology*, 82, 407-408.
- Grove, T.L., Baker, M.B., and Kinzler, R.J. (1984) Coupled CaAl-NaSi diffusion in plagioclase feldspar: Experiments and applications to cooling rate speedometry. *Geochimica et Cosmochimica Acta*, 48, 2113-2121.
- Kouchi, A., and Sunagawa, I. (1985) A model for mixing basaltic and dacite magmas as deduced from experimental data. *Contributions to Mineralogy and Petrology*, 89, 17-23.
- Koyaguchi, T. (1985) Magma mixing in a conduit. *Journal of Volcanology and Geothermal Research*, 25, 365-369.
- Kuo, L.-C., and Kirkpatrick, R.J. (1982) Pre-eruption history of phryic basalts from DSDP Legs 45 and 46: Evidence from morphology and zoning patterns in plagioclase. *Contributions to Mineralogy and Petrology*, 79, 13-27.
- Lofgren, G.E. (1974) Temperature-induced zoning in synthetic plagioclase feldspar. In W.S. Mackenzie and J. Zussman, Eds., *The feldspars*, p. 362-375. Manchester University Press, Manchester.
- (1980) Experimental studies on the dynamic crystallization of silicate melts. In R.B. Hargraves, Ed., *Physics of magmatic processes*. Princeton University Press, Princeton, New Jersey.
- Lofgren, G.E., and Norris, P.N. (1981) Experimental duplication of plagioclase sieve and overgrowth textures. *Geological Society of America Abstracts with Programs*, 13, 498.
- Loomis, T.P. (1981) An investigation of disequilibrium growth processes of plagioclase in the system anorthite-albite-water by methods of numerical simulation. *Contributions to Mineralogy and Petrology*, 76, 196-205.
- (1982) Numerical simulations of crystallization processes of plagioclase in complex melts: The origin of major and oscillatory zoning in plagioclase. *Contributions to Mineralogy and Petrology*, 81, 219-229.
- Loomis, T.P., and Welber, P.W. (1982) Crystallization processes in the Rocky Hill granodiorite pluton, California: An interpretation based on compositional zoning of plagioclase. *Contributions to Mineralogy and Petrology*, 81, 230-239.
- MacDonald, G.A., and Katsura, T. (1965) Eruption of Lassen Peak, Cascade Range, California in 1915: Example of mixed magmas. *Geological Society of America Bulletin*, 76, 475-482.
- Morrice, M.G., and Gill, J.B. (1986) Spatial patterns in the mineralogy of island arc magma series: Sangihe arc, Indonesia. *Journal of Volcanology and Geothermal Research*, 29, 311-353.
- Morse, S.A. (1979) Influence of augite on plagioclase fractionation. *Journal of Geology*, 87, 202-208.
- (1984) Cation diffusion in plagioclase feldspar. *Science*, 225, 504-505.
- Nixon, G.T. (1987) Contributions to the geology and petrology of the Trans-Mexican volcanic belt. Ph.D. thesis, University of British Columbia, Vancouver, British Columbia.
- Nixon, G.T., Demant, A., Armstrong, R.L., and Harakal, J.E. (1987) K-Ar and geologic data bearing on the age and evolution of the Trans-Mexican volcanic belt. *Geofisica Internacional*, 26, 109-158.
- Pearce, T.H. (1984a) Multiple frequency laser interference microscopy: A new technique. *The Microscope*, 32, 69-81.
- (1984b) Optical dispersion and zoning in magmatic plagioclase: Laser-interference observations. *Canadian Mineralogist*, 22, 383-390.
- Rhodes, J.M., Dungan, M.A., Blanchard, D.P., and Long, P.E. (1979) Magma mixing at mid-ocean ridges: Evidence from basalts drilled near 22°N on the Mid-Atlantic Ridge. *Tectonophysics*, 55, 35-61.
- Sibley, D.F., Vogel, T.A., Walker, B.W., and Byerly, G. (1976) The origin of oscillatory zoning in plagioclase: A diffusion and growth controlled model. *American Journal of Science*, 276, 275-284.
- Smith, J.V. (1974) Feldspar minerals, vol. 2, Chemical and textural properties. Springer-Verlag, Berlin.
- Smith, R.K., and Lofgren, G.E. (1983) An analytical and experimental study of zoning in plagioclase. *Lithos*, 16, 153-168.
- Tsuchiyama, A. (1985) Dissolution kinetics of plagioclase in the melt of the system diopside-albite-anorthite, and origin of dusty plagioclase in andesites. *Contributions to Mineralogy and Petrology*, 89, 1-16.
- Vance, J.A. (1965) Zoning in igneous plagioclase: Patchy zoning. *Journal of Geology*, 73, 636-651.
- Walker, D., Kirkpatrick, R.J., Longhi, J., and Hays, J.F. (1976) Crystallization history of lunar picrite basalt sample 12002: Phase equilibria and cooling rate studies. *Geological Society of America Bulletin*, 87, 646-656.
- Walker, D., Shibata, T., and DeLong, S.E. (1979) Abyssal tholeiites from the Oceanographer fracture zone. II. Phase equilibria and mixing. *Contributions to Mineralogy and Petrology*, 70, 111-125.
- Yoder, H.S., and Tilley, C.E. (1962) Origin of basalt magmas: An experimental study of natural and synthetic rock systems. *Journal of Petrology*, 3, 342-532.

## APPENDIX 1. PHENOCRYST ZONING PROFILES

Descriptions of phenocryst zoning profiles shown in Figures 7 to 9 are given below in terms of four principal attributes: (1) phenocryst rims (i.e., the inclusion-free region outside discontinuity 1); (2) inclusion zones; (3) compositional hiatuses across discontinuities; and (4) zoning following resorption. Discontinuities are numbered sequentially from the margin of the phenocryst, and regions of interest are referenced as, for example, P3-1: D1–D2, which designates the region in profile P3-1 between discontinuities 1 and 2.

### Mixed lava P3 (Fig. 7)

**Phenocryst rims.** Normally zoned calcic overgrowths (3–50  $\mu\text{m}$  thick) vary in composition from  $\text{An}_{64}$  to  $\text{An}_{48}$  at discontinuity 1 to  $\text{An}_{50}$  to  $\text{An}_{44}$  at the edge of the crystal. The latter variation is attributed to difficulties experienced in locating precisely the fringe terminations and possible edge effects (e.g., crystal margins inclined to the plane of section may accentuate the extent of normal zoning). Microlite cores ( $\text{An}_{56}$ – $\text{An}_{48}$ ) are similar to bulk rim compositions but are slightly more sodic than the maximum An content of these rims as inferred from the fringe pattern. This difference is corroborated by microprobe analysis, which, despite the greater volume of material sampled by the electron beam, gives compositions of  $\text{An}_{60}$  at the inner rim of P3-5.

**Inclusion zones.** Sieve textures are enclosed by clear calcic rims and exhibit an inner corrosive surface (discontinuity 1) where relict zoning is locally preserved (e.g., P3-6). Inclusions appear to have been trapped primarily during growth (P3-2), and coarse sieve textures are found within some cores (P3-7).

**Discontinuities.** Compositional hiatuses range from 3 to 33 mol%  $\Delta X_{\text{An}}$ . The change in composition across discontinuity 1 varies from 14 to 28 mol% An and jumps of 10–20 mol% occur internally within all zoning profiles.

**Postresorption zoning.** Zoning after resorption is usually normal or oscillatory-normal, and rarely even (e.g., P3-4: D4–D5 and D5–D6), reverse or oscillatory-reverse (e.g., P3-3: D6–D7 and P3-6: D9–D10). Linear normal zoning between discontinuities may be extensive (e.g.,  $\text{An}_{63}$ – $\text{An}_{28}$  in P3-3: D7–D8).

### Hornblende dacites R1, R3 (Fig. 8)

**Phenocryst rims.** Calcic overgrowths generally range in width from 5 to 20  $\mu\text{m}$ . Zoning is commonly normal and weakly oscillatory in the thicker rims (20  $\mu\text{m}$ ). The inner rim varies from  $\text{An}_{64}$  to  $\text{An}_{55}$  and decreases outward to the mean bulk phenocryst composition ( $\text{An}_{40}$ ).

**Inclusion zones.** Inclusions are typically concentrated proximally to resorption surfaces. Many such zones exhibit corroded internal margins overgrown by more calcic plagioclase, but the nature of inner zone boundaries is not definitive in every case.

**Discontinuities.** Discontinuity 1 often retains a strong morphological expression of dissolution (e.g., fritted margins excavated  $\parallel$  (010), rounding of corners) regardless of the composition of rim overgrowths. Crystals with calcic rims record changes in An content across discontinuity 1 of 10–24 mol%, and discontinuities  $\geq 10$  mol% An occur in every profile. Rarely, resorption surfaces are overlain by Na-rich zones (R1-2: D2–D3 and D6–D7; Figs. 5C, 5D).

**Postresorption zoning.** Steep normal zoning is common in the most calcic rims, normal or oscillatory-normal zoning at internal discontinuities, and rarely even (R1-3: D5–D6) and reverse zoning (R1-2: D2–D3 and D6–D7). Linear normal zoning is observed locally (e.g., R1-3: D2–D3).

### Mixed lavas R9, P1, P4, P15 (Fig. 9)

**Phenocryst rims.** Calcic overgrowths generally range in width from 5 to 30  $\mu\text{m}$ . Rare subhedral to euhedral phenocrysts may lack calcic rims either locally (re-entrant thinning) or entirely. Anhedral phenocrysts lacking such overgrowths have not been observed. Inner rim compositions peak at about  $\text{An}_{66}$  (P4-2, P4-3) but are variable and extend down to  $\text{An}_{44}$  (P1). Zoning toward the edge terminates as low as  $\text{An}_{37}$  (P1) but is commonly greater than  $\text{An}_{48}$ . The calcic rim is similar to the composition of microlite cores (except P1), though zoning in the rim of some phenocrysts appears to start at higher An contents (e.g., P4). In P15-3, the composition of the calcic overgrowth appears to vary laterally from  $\text{An}_{51}$  on one side of the phenocryst where the rim is thin (10–15  $\mu\text{m}$ ) to  $\text{An}_{61}$  on the opposite side where the rim is thicker (25  $\mu\text{m}$ ).

**Inclusion zones.** Sieve textures (10–60  $\mu\text{m}$  in width) are commonly bracketed by destructive (discontinuity 1) and constructional (calcic rim) interfaces.

**Discontinuities.** Although compositional hiatuses across resorption surfaces ( $\Delta X_{\text{An}} = 3$  to 32 mol%) commonly reach a maximum at discontinuity 1, major internal breaks ( $\Delta X_{\text{An}} \geq 10$  mol%) are evident in all profiles and may even exceed the hiatus at the rim (e.g., P1).

**Postresorption zoning.** The most common style of zoning immediately succeeding resorption is normal or normal-oscillatory; uniform compositions are less frequently encountered (e.g., P4-2: D2–D3), and reverse zoning is rare (e.g., P15-3: D4–D5; P15-2: D2–D3, D4–D5, D5–D6). Continuous linear zoning is also observed (e.g., P4-1: D4–D5 and R5 rim in Figs. 4C, 4D).